



## Sand invasion along the Portuguese coast forced by westerly shifts during cold climate events

Susana Costas<sup>a,\*</sup>, Sonia Jerez<sup>b</sup>, Ricardo M. Trigo<sup>b,c</sup>, Ronald Goble<sup>d</sup>, Luís Rebêlo<sup>a</sup>

<sup>a</sup> *Unidade de Geologia Marinha, LNEG, 7586, Alfragide, 2610-999 Amadora, Portugal*

<sup>b</sup> *Instituto Dom Luiz, Universidade de Lisboa, 1749-016 Lisboa, Portugal*

<sup>c</sup> *Departamento de Engenharias, Universidade Lusófona, 1749-024 Lisboa, Portugal*

<sup>d</sup> *Department of Earth and Atmospheric Sciences, University of Nebraska, Lincoln, NE 68588-0340, USA*

### ARTICLE INFO

#### Article history:

Received 19 December 2011

Received in revised form

13 March 2012

Accepted 17 March 2012

Available online 25 April 2012

#### Keywords:

Cliff-top dunes

OSL

GPR

Westerlies

Portugal

Paleoclimate

NAO

Storminess

### ABSTRACT

Phases of higher aeolian activity are responsible for the formation and movement of large transgressive dunefields. Well-reported phases of aeolian activity in northwest Europe are coincident with global cooling events and were related to enhanced westerly winds and storminess. However, the extent to which these climatic episodes influenced dunefield dynamics in southwest Europe remains an open question. Ground penetrating radar (GPR) was used to image the stratigraphy of a cliff-top coastal transgressive dunefield in Portugal and reconstruct former windfield regimes. Using optically stimulated luminescence (OSL) five major phases of aeolian activity were dated at 12.6, 5.6, 1.2, 0.4 and 0.3 ka, and related to coastal instability and enhanced westerlies. These phases were later reconciled to favorable patterns of atmospheric circulation simulated by global and regional climate models at both synoptic and local scales, respectively. The results prove that major phases of aeolian activity in southwest Europe are associated with the onset of cold climate events of global distribution coinciding with aeolian accumulation in northwest Europe. This implies the dominance of zonal westerlies along the western coast of Europe from Denmark to Portugal during the onset of cold climate events. Model simulations suggest that the pattern of atmospheric circulation during periods of enhanced aeolian activity is compatible with prolonged negative phases of the North Atlantic Oscillation (NAO).

© 2012 Elsevier Ltd. All rights reserved.

### 1. Introduction

Environmental conditions during the end of the last glacial created the necessary conditions to trigger the formation of coversands in northwest and central Europe (Kasse, 2002; Renssen et al., 2007). The occurrence of coversands is patchy in Great Britain (Bateman, 1995) but on the continent the coversands form an extended latitudinal belt of continuous deposits including The Netherlands, Germany, Denmark, Poland and Russia (Zeeberg, 1998; Schirmer, 1999). However, significant aeolian activity in Europe was not restricted to the north of the continent. The accumulation of large dunefields was assigned to this time period in the south-west coast of France (Bertran et al., 2009), center of Spain (Bateman and Díez Herrero, 2001; García-Hidalgo et al., 2007), and some areas of the Portuguese (Ramos Pereira and Angelucci, 2004; Granja et al., 2008; Danielsen et al., 2011) and Atlantic Spanish coasts (Zazo et al., 2005). The synchronous character of aeolian accumulation along Europe suggests a common driving factor during the end of the

last glacial. The climate has been repeatedly referred to as responsible for the formation of these aeolian deposits by changing the patterns of atmospheric circulation and thus sparseness of vegetation cover (Kasse, 2002). However, more information regarding the temporal and spatial resolution of the aeolian record is needed to better understand the palaeoclimatic implications of aeolian activity in the northeast Atlantic Basin. In this line, we will first investigate the circulation mode from the aeolian record of Caparica in Portugal by combining high-resolution Ground Penetrating Radar (GPR) images of the subsurface and Optically Stimulated Luminescence (OSL) ages. Then, making use of our current knowledge on atmospheric dynamics, proxy-based reconstructions will be reconciled with mesoscale and regional models of atmospheric circulation in an attempt to investigate the windfield regimes responsible for aeolian sand accumulation in the past.

#### 1.1. The Portuguese littoral belt

The Portuguese coast extends for more than 900 km, of which 60% are beaches and 36% contain cliffs without beaches (Andrade

\* Corresponding author.

E-mail address: [susana.costas@lneg.pt](mailto:susana.costas@lneg.pt) (S. Costas).

et al., 2002). Currently, 28% of the coast experiences severe problems of erosion (Eurosion, 2004). Despite the starved character of the present Portuguese shoreline, large stabilized transgressive dunefields dominate the coast. These deposits document periods of significant sediment availability within the littoral system contributing to the formation of the Portuguese littoral belt since Middle Pleistocene (Ramos Pereira and Angelucci, 2004). The Portuguese littoral belt is formed by consolidated and non-consolidated dunes. The consolidated dunes have been described and tentatively interpreted and dated by Ramos Pereira and Angelucci (2004). However, references to the non-consolidated transgressive dunes are sparse and poorly developed despite their larger spatial distribution. The oldest non-consolidated dunes within the Portuguese coast were dated at 30,000 to 23,000 cal yr BP in San Pedro de Maceda beach, central region of Portugal (Granja et al., 2008). Later, successive phases of dune building were dated within that coastal segment (Clarke and Rendell, 2006; Granja et al., 2008; Danielsen et al., 2011). The occurrence of sand drift and dune building episodes along the Portuguese coast has been related to changes in vegetation cover, water table and storminess induced by changing climatic conditions (Clarke and Rendell, 2006; Granja et al., 2008). The most recent episode of coastal dune building in Portugal was related to increased storminess during the Little Ice Age (LIA) and was coincident with a broader episode of dune construction in western European coasts (Clarke and Rendell, 2009). However, comprehensive investigations have shown different pulses of aeolian activity occurring at different time intervals depending on their latitude. Clarke and Rendell (2006) dated dune accumulation in France at AD 1452–1752, while in Portugal they documented aeolian sand movement at AD 1770–1905. The authors interpreted this latitudinal out of phase as reflecting different Atlantic storm tracks driven by changes in the prevailing state of the North Atlantic Oscillation pattern (hereafter NAO). They linked aeolian activity in Portugal to increased storminess associated to predominantly negative winter NAO as reconstructed by Luterbacher et al. (2002), while in France dune building and thus increased storminess occurred under predominantly positive winter NAO.

The present conditions for aeolian activity in the Portuguese coast contrasts with the environmental conditions which generated the ancient Portuguese littoral belt. The occurrence of active dunefields along the Portuguese coast is nowadays very rare with the exception of locations with orographically induced strong winds. Orography may locally provoke intensification of onshore winds which maintain active dunefields such as the case of the Guincho-Oitavos dunefield (Rebêlo et al., 2002). However, the vast majority of the coastal dunes are nowadays either stabilized or eroding. This fact provides additional interest on the understanding of these ancient aeolian deposits as they may record contrasting environmental conditions or even different degrees of human pressure. In this context, a number of questions regarding the occurrence of recent phases of aeolian activity in Portugal remain unanswered: (i) what are the specific conditions triggering historic and older pulses of aeolian activity along the Portuguese coast? (ii) to what extent has human pressure influenced the occurrence of aeolian transgressive pulses? or (iii) what is the significance of the dune building phases within the broader regional or even global context?

This work explores the aeolian pulses in the Portuguese coast as a contribution to the overall understanding of the significance of these episodes in a local and global scale as potential environmental indicators. An aeolian coversand around 42 km<sup>2</sup> was explored in order to identify the different pulses of dune building. The selected study area consists of a cliff-top dunefield located in Capararica, in the Lisbon region of Portugal facing the western open ocean coast.

## 2. Physiographic settings

### 2.1. The cliff-top dunefield

Caparica cliff-top dune is a transgressive dunefield located within the western-central sector of the Setúbal Peninsula, about 20 km south of Lisbon, in the Portuguese Atlantic Coast. This transgressive dunefield developed on top of a terrace located around 50 m above mean sea-level (MSL). They can be considered as perched dunes formed on top of pre-existing geological formation. The dunefield extends up to 4.5 km inland from the edge of the cliff and is 42 km<sup>2</sup> in areal extent. The coastal segment located in the base of the cliff is characterized by a 25 km long coastal plain which stretches to the south (Fig. 1). The physical boundaries of the coastal plain are represented inland by a coastal cliff section 100–55 m high. The cliff consists of unconsolidated deposits interpreted by Azevedo (1983) as fluvial sediments deposited during the Pliocene and corresponding to the landward Tagus paleo-valley. To the north, the coastal plain is limited by the Tagus inlet and ebb-delta, whereas the consolidated Espichel Cape constitutes the southern limit (Fig. 1). The abandoned cliff is protected from wave attack by the coastal plain to the north. However, sub-aerial denudation reduces the slope of the cliff with its upper edge more indented. By contrast, the cliff is being actively eroded to the south where winter waves used to reach the toe of the cliff. The northern part of the coastal plain has experienced significant human pressure during the last decades, which generated serious problems of erosion and properties destruction. Subsequently, different actions have been carried out to prevent further erosion including artificial nourishment and shoreline armoring. The central section of the littoral arc, north of Fonte da Telha beach (Fig. 1), is characterized by two distinctive foredune fields. The inland foredune, reaching up to 200 m in width, is colonized by a well-developed forest which was planted in the end of the 20th century to steady dunes. The seaward foredune is around 80 m width and fixed by *Ammophila* sp. Both dunefields may reach 12 m height. Contrasting with these low relief dunefields, the transgressive perched dunes comprise very large dune buildings that may reach up to 30 m height (Costas et al., 2010). The first attempt to place cliff-top dune formation in a geographically-temporal framework was made by Antunes and Pais (Antunes and Pais, 1989) who dating organic horizons situated dune formation around 1190 ± 90 yr BP.

### 2.2. The climate

The study area is dominated by the typical Mediterranean climate type with mild and relatively wet winters followed by dry and hot summers. However, being located on the western Iberian Atlantic coast, and at this latitude (~39°N), the study area is under the influence of both tropical and mid-latitude climate dynamics. As a transition zone between these two regimes it is very sensitive to changes of their relative strength and geographical extension. This helps to explain why the climate of Iberia is particularly sensitive to global climate change, as shown by trends and high variability at both short (decadal) and long (millennial) time scale in past records (Trigo et al., 2006). According to the latest IPCC report (2007), the Mediterranean basin (including western Iberia) appears to be particularly prone to suffer a significant warming and decrease in precipitation during the 21st century and is now widely regarded as the most important “hot spot” of climate change in the world (Giorgi, 2006).

Despite this complexity, the climate of western Iberia is dominated by just a few large-scale atmospheric circulation patterns or teleconnections (Trigo et al., 2008). Among these, it is now widely recognized that the most important teleconnection

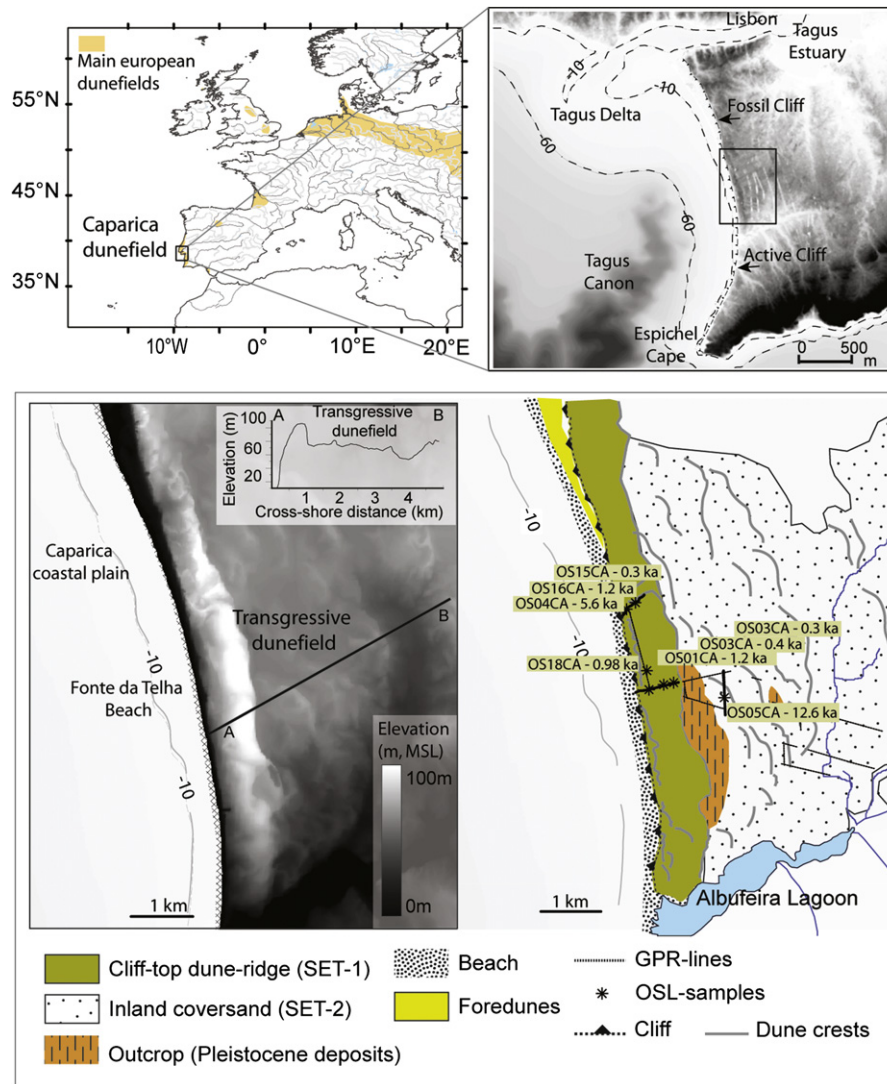


**Fig. 1.** Upper panel shows in orange the coverage of the coversand sheet of northwest Europe (Kasse, 1997), southern France (Bertran et al., 2009), northern Portugal (Granja et al., 2008) and the location of the study area, the Caparica dunefield in Portugal. The left lower panel shows the terrain elevation model (TEM) of the study area where the cliff-top dune ridge and the inland sand-sheet are visible. The lower right panel shows the TEM interpretation and location of the sampling for OSL and GPR. (For interpretation of the references to colour in this figure legend, the reader is referred to the web version of this article.)

corresponds to the NAO pattern that controls a large amount of climate variability of western Europe, especially during wintertime (Hurrell, 1995). The NAO pattern is characterized by a meridional gradient in sea-level pressure over the North Atlantic; high pressures dominating west of Iberia in the Atlantic sector around the Azores Islands (Azores High), and frequent low pressure systems over northern regions near Iceland (Iceland Low). This dipolar pattern is enhanced during positive phases of NAO and weakened during negative NAO phases (Jones et al., 1997). On inter-annual and shorter time scales, the NAO dynamics can be explained as a purely internal mode of variability of the atmospheric circulation. Interdecadal variability may be influenced, however, by ocean and sea-ice processes (Wanner et al., 2001). The positive and negative phases of the NAO mode are accompanied by different spatial patterns of precipitation (Trigo et al., 2004). During high NAO index winters, drier conditions occur over much of central and southern Europe, whereas enhanced moisture flux convergence occurs from Iceland through Scandinavia (Hurrell, 1995). These circumstances are marked by an increase in cyclone frequency, enhanced westerlies across the northern North Atlantic

and an increase of winter air temperatures (Trigo et al., 2002). Conversely, enhanced storminess and precipitation between the Azores archipelago and Iberia were documented during episodes of strongly negative index values (Trigo et al., 2004; Vicente-Serrano et al., 2011). However, relatively high storminess in the northern North Atlantic has been documented associated with low values of monthly NAO index or even strongly negative values (Dawson et al., 2002).

Similarly to most of the Mediterranean basin region, the distribution of precipitation in Portugal exhibits a marked seasonal character with a strong contrast occurring between a 'dry season', with almost no rainfall during the months of July and August, and a wetter period throughout the rest of the year. Moreover, the precipitation regime reveals a marked inter-annual variability with relatively high probabilities of occurrence of wet and dry years. At the monthly and seasonal temporal scales the high inter-annual variability of precipitation is mostly controlled by the NAO pattern. Winds are clearly dominated by northerlies (48%), while westerly and southwesterly winds explain around 17% of the windfield in the area (Alcoforado, 1992). This pattern is almost

constant during the year with an increase of the occurrence of northerly winds towards summer months.

### 3. Methodology

The dunefield was mapped and morphologically characterized using georeferenced geological maps and aerial photographs dating to 1958. This information was decisive on the planning of the geophysical exploration of the dunefield. In addition, a simulation of the atmospheric circulation was assessed to reconstruct the wind regimes inducing the onset of the large-scale transgressive dunefield using dynamically downscaled windfield at both, local-high resolution and synoptic scales.

#### 3.1. The stratigraphy of the dunefield

GPR has been successfully used to image the internal stratigraphy of desert and coastal dunes as their sediments have low conductivity and contain large-scale sedimentary structures that can be imaged and differentiated by GPR (Bristow, 2009). An IDS–GPR system RIS MF Hi-Mod #1 using a dual frequency antenna (200 and 600 MHz) was used to acquire more than 10 km of subsurface images. The system was synchronized to a RTK–GPS system in order to obtain the topographical information for static correction during the processing of the radargrams. Raw data were processed using the program package Reflex-Win Version 5.0.5 by Sandmeier Software. Processing included time-zero drift, application of filters and gains, velocity profile estimates, migration and static corrections. An average subsurface velocity of 0.16 m/ns was estimated using the interactive hyperbola-adaptation method and was a typical velocity for dry sand.

The radar images were interpreted using Kingdom Software in order to obtain the spatial coverage of the identified radar units. Radar units were defined by the occurrence of first-order surfaces. Additionally, super-surfaces were identified and supported by field characterization. Super-bounding surfaces in the sense of Kocurek (1991) reflect the prevailing conditions during a hiatus period in dunefield accumulation, which switch from favorable for accumulation to unfavorable. Therefore, they can be used as a basis for event stratigraphy as they cap a genetic sequence in an area.

#### 3.2. Chronology of aeolian activity

Sample collection was designed on the basis of the radar images and interpretation. This information allowed dating major depositional units. All the samples were taken from the undisturbed original sediments.

#### 3.2.1. Sample preparation and dose-rate determination

Sample preparation was carried out under amber-light conditions. Samples were wet sieved to extract the 150–250  $\mu\text{m}$  fraction, and then treated with HCl to remove carbonates. Quartz and feldspar grains were extracted by flotation using a 2.7  $\text{g cm}^{-3}$  sodium polytungstate solution, then treated for 60 min in 48% HF, followed by 30 min in 47% HCl. The sample was then re-sieved and the <150  $\mu\text{m}$  fraction discarded to remove residual feldspar grains. The etched quartz grains were mounted on the innermost 2 mm or 5 mm of 1 cm aluminum disks using Silkospray. Chemical analyses were carried out using a high-resolution gamma spectrometer. Dose-rates were calculated using the method of (Aitken, 1998) and (Adamiec and Aitken, 1998). The cosmic contribution to the dose-rate was determined using the techniques of (Prescott and Hutton, 1994).

#### 3.2.2. Optical measurements

Optically stimulated luminescence analyses were carried out on Riso Automated OSL Dating System Model TL/OSL-DA-15B/C and TL/OSL-DA-20 readers, equipped with blue and infrared diodes, using the Single Aliquot Regenerative Dose (SAR) technique (Murray and Wintle, 2000). All the values were determined using the Central Age Model (Galbraith et al., 1999), unless data analysis using the decision table of Bailey and Arnold (2006) indicated partial bleaching (UNL3022 and 3023, Table 1), in which case the Minimum Age Model (Galbraith et al., 1999) was used. Preheat and cutheat temperatures were based upon preheat plateau tests between 180° and 280 °C. A preheat of 200 °C was used for samples UNL3021, 3022, and 3023, and a preheat of 240 °C for samples UNL3024 and 3025. Dose-recovery and thermal transfer tests were conducted (Murray and Wintle, 2003). Growth curves were examined to determine whether the samples were below saturation ( $D/D_0 < 2$ ; Wintle and Murray (2006)). Optical ages are based upon a minimum of 50 aliquots. Individual aliquots were monitored for insufficient count-rate, poor quality fits (i.e. large error in the equivalent dose,  $D_e$ ), poor recycling ratio, strong medium vs fast component (Durcan et al., 2009), and detectable feldspar. Aliquots deemed unacceptable based upon these criteria were discarded from the dataset prior to averaging. Averaging was carried out using the Central Age Model (Galbraith et al., 1999) unless the  $D_e$  distribution (asymmetric distribution; skew  $> 2\sigma_c$ , Bailey and Arnold (2006)), indicated that the Minimum Age Model (Galbraith et al., 1999) was more appropriate.

#### 3.3. Wind regime simulations

The assessment of the impact of the NAO mode on the near surface windfield was performed using two distinct databases of atmospheric variables, both spanning between 1959 and 2007. At

**Table 1**  
Luminescence dating results (OSL ages in years before 2010).

UNL#	Sample	Burial depth (m)	H <sub>2</sub> O (%) <sup>a</sup>	K <sub>2</sub> O (%)	U (ppm)	Th (ppm)	Cosmic (Gy)	Dose Rate (Gy/ka)	D <sub>e</sub> (Gy) <sup>b</sup>	Aliquots	Age(ka)
UNL3021	OS01CA-2010	1	0.9		0.74	2.04	0.18	1.65 ± 0.06	2.01 ± 0.05	56	1.22 ± 0.05
UNL3022	OS02CA-2010	1.5	1.1		0.78	2.73	0.17	1.68 ± 0.06	0.97 ± 0.04	55	0.58 ± 0.03
	Minimum Age Model (Galbraith et al. 1999)								0.74 ± 0.03		0.44 ± 0.02
UNL3023	OS03CA-2010	1	1.5		0.75	2.51	0.18	1.79 ± 0.06	0.72 ± 0.36	57	0.40 ± 0.20
	Minimum Age Model (Galbraith et al. 1999)								0.54 ± 0.03		0.30 ± 0.02
UNL3024	OS04CA-2010	1	0.4		1.32	4.68	0.18	2.24 ± 0.08	12.50 ± 0.15	57	5.57 ± 0.21
UNL3025	OS05CA-2010	0.8	2.8		0.78	2.01	0.19	1.51 ± 0.06	18.97 ± 0.58	58	12.6 ± 0.6
UNL3399	OS15CA-2011	1.20	2.29	1.44	0.71	1.97	0.15	1.55 ± 0.06	1.04 ± 0.12	59	0.67 ± 0.08
	Minimum Age Model (Galbraith et al. 1999)								0.54 ± 0.04		0.35 ± 0.03
UNL3400	OS16CA-2011	1.08	0.74	1.69	0.73	1.91	0.18	1.78 ± 0.06	3.69 ± 0.27	56	2.08 ± 0.17
	Minimum Age Model (Galbraith et al. 1999)								2.05 ± 0.06		1.15 ± 0.06
UNL3402	OS18CA-2011	0.94	0.25	1.74	0.55	1	0.18	1.77 ± 0.06	1.74 ± 0.05	51	0.98 ± 0.05

<sup>a</sup> In-situ Moisture Content.

<sup>b</sup> Central Age Model (Galbraith et al., 1999) unless otherwise indicated choice of age model is based upon decision table of Bailey and Arnold (2006).

the lower resolution ( $1.125^\circ \times 1.125^\circ$ ), suitable for resolving synoptic scale features, we used the ERA-40 Reanalysis dataset (Uppala et al., 2005) from the European Centre for Medium Range Weather Forecast (ECMWF) available between 1959 and 2002 and complemented until 2007 by the corresponding Analysis forecasts. At higher resolution (10 km)-regional scale, we used a hindcasted database obtained by dynamically downscaling the former data over the entire Iberian Peninsula using the mesoscale model MM5 (Grell et al., 1995). For further details of the simulation and its accuracy the reader is referred to Lorente-Plazas (2010).

The monthly values of the NAO index for the period 1959–2007 were obtained from the Climate Prediction Center (CPC) from the National Oceanic and Atmospheric Administration (NOAA) (<http://www.cpc.ncep.noaa.gov/data/teleodoc/telecontents.shtml>). Following the approach employed in Trigo et al. (2008), we defined classes of positive (NAO+ if  $\text{NAO} > 0.5$ ) and negative (NAO- if  $\text{NAO} < -0.5$ ) phases of NAO, with the remaining months corresponding to the normal class. The study of the NAO impact is then addressed by comparison of the mean fields (namely, sea-level pressure and wind module and direction at 10 m height above the sea-level) for months with NAO+ and NAO-. Finally, the monthly results are grouped, for the sake of brevity, into the extended winter (ONDJFM) and summer (JJA) seasons that takes into account the large intra-annual variability and level of similarity among different months. A total of 84 (55) winter (summer) months with positive NAO, and 111 (33) winter (summer) months with negative NAO, were averaged in each case.

## 4. Results

### 4.1. Dunefield morphology and architecture

The complementary analysis of aerial photographs, digital terrain models and the internal stratigraphy of the dunes, suggests

very complex dune morphology and evolution. The various dune-crests indicate the occurrence of several pulses of aeolian activity (Fig. 1). The dunefield was divided in two major sets or dune grouping regarding the geometry and spatial distribution of the dunes (Fig. 1). A dense vegetation cover, including forest exploration, stabilizes the dunefield at present.

#### 4.1.1. The cliff-top dune-ridge (SET-1)

The first set (SET-1) is represented by a dune ridge reaching 100 m above MSL landward of the edge of the cliff, which is already 50 m above MSL. The dune ridge is classified following the nomenclature proposed by Wolfe and David (1997) as a merged dune included within the compound parabolic dunes type. The ridge is 700 m wide and extends along 8 km parallel to the edge of the cliff. The northern extreme of the ridge is degraded showing isolated crest remnants of earlier dune arms or digitate parabolic dunes. The presence of this ridge suggests that individual parabolic dunes moved simultaneous to merge into a unique ridge.

Three radar units were identified within the ridge (Figs. 2 and 3). Isolated remains of the lowermost radar unit (U1) suggest low preservation during the early stages of accumulation of the cliff-top dune (Fig. 2). U2 overlays U1 to the north (Fig. 2) and the partially consolidated fluvial deposits, comprising the underlying Pleistocene deposits, to the south (Fig. 3). A high-amplitude reflection interpreted as a super-surface (H1) was identified to the top of U1 suggesting the cessation of aeolian sedimentation and very likely the sub-aerial exposure of U1 (Fig. 2). U2 comes to the surface in cross line SET1-01 where it was sampled for OSL dating. Internally, U2 presents a complex organization with numerous subunits, which dimensions range from 140 to 350 m long and 2–10 m thick. Subunits are defined by concave-up bounding surfaces. Reflections within the subunits show variable configurations, from subhorizontal and hummocky reflections to oblique clinofolds dipping either northwards or southwards.

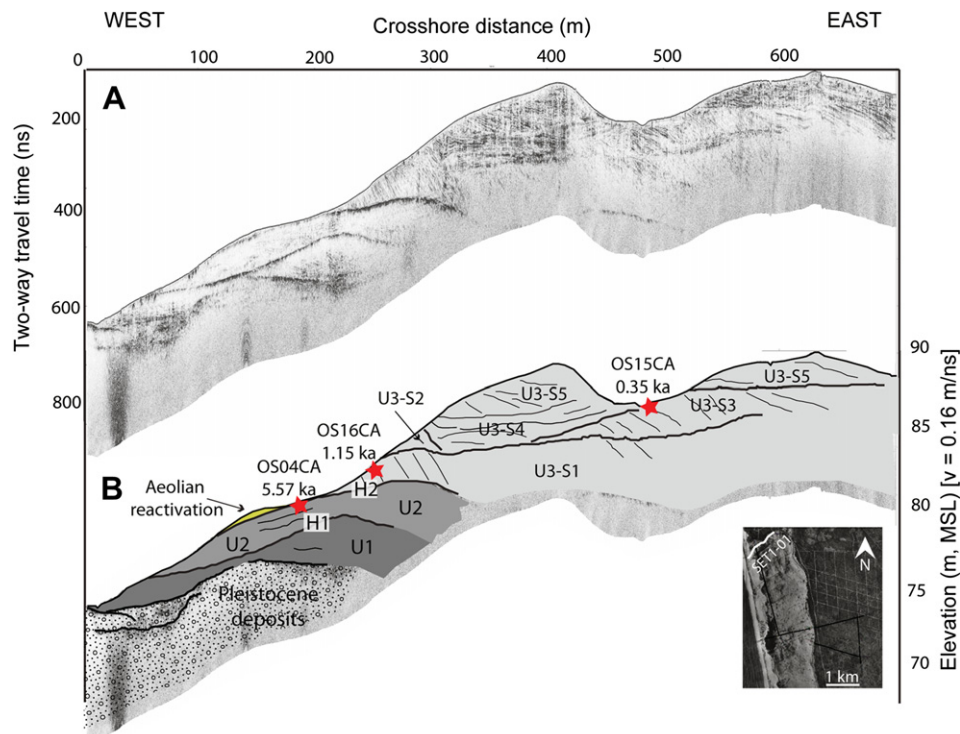


**Fig. 2.** (A) West–east directed GPR profile SET1-01. (B) Interpretation of the radargram with the identified radar units. The location of the sediment samples for dating the radar units is also pointed as well as the resulting ages.

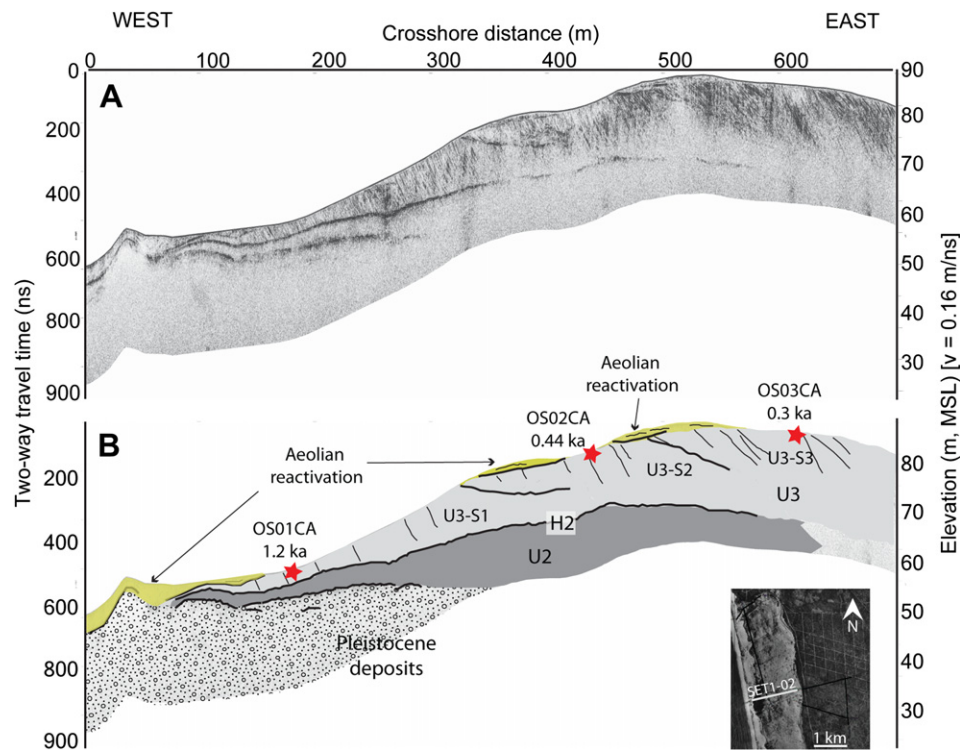


**Fig. 3.** (A) West–east directed GPR profile SET1-02. (B) Interpretation of the radargram with the identified radar units. The location of the sediment sample for dating the radar units is also pointed as well as the resulting ages.

The sediments are characterized by well-sorted medium to coarse sand dominated by grains of quartz and a very low content of feldspar. The bottom of this unit is characterized by a discontinuous high-amplitude reflection with abundant hyperbolas that can be attributed to the irregular surface and abundant gravels and cobbles of the underlying Pleistocene deposits. The upper boundary of U2 is defined by super-surface H2 (Figs. 2 and 3); a high-amplitude and continuous double-reflector with abundant hyperbolas. H2 is formed by gray sediments (fine sand and clays) partially consolidated. Super-surface H2 suggests that U2 was fixed and sub-aerially exposed before being buried by new aeolian sands contributing to the vertical growth of the ridge. The abundant hyperbolas associated to this reflector may support the very likely sub-aerial weathering.

U2 is overlain by radar unit U3, which can be divided into multiple radar packages or subunits delimited by superimposition surfaces (Figs. 2 and 3). U3 is dominated by oblique parallel clinoforms dipping 23° landward. This configuration represents former positions of the slipface and is interpreted as resulting from grainfall deposition. Windward of the preserved crest, the lee-slope geometry is replaced by moderate to low-angle cross-stratification, interpreted as grainflow deposition. Hugenholtz et al. (2008) attributed changes in the geometry of the dunes to variations in sand supply, which in turn determine vegetation development and sedimentation processes along the crest and lee-slope. Therefore, dunes with reduced crest/brink separation would be dominated by grainfall deposition and high sand supply. In the present case, the change in the geometry of the subunits from a high- to a low-angle slipface is interpreted as the terminal growth phase of the dune. The rearrangement on the dune geometry could result from a decline of sand input as wind strength decays, which is followed by a temporal interruption in aeolian activity. Alternatively, the internal configuration of Unit-3 imaged in a longitudinal line showed diverse internal configurations; subhorizontal patterns to

oblique clinoforms dipping up to 8° to the south. More rarely, northward dipping reflections can be also documented. The dimensions of the subunits range between 100 and 900 m and are bounded by concave-up surfaces imaged within the longitudinal GPR profile.

#### 4.1.2. The inland coversand (SET-2)

The second set (SET-2) of parabolic dunes extends over a larger surface, with 2.2 km length and at least 5 km width inland of SET-1 (Fig. 1). SET-1 and 2 appear separated by Pleistocene deposits outcropping along the base of the dune-ridge slipface (Fig. 1). Yet, we cannot discard the presence of dune remains of SET-2 underneath SET-1 (i.e. U1). The partial destruction of the dunefield by human occupation prevents the identification of the entire set to the north. This second dune set is represented by partially-filled to filled superimposed parabolic dunes. U-shaped depressions were originated from blowout erosion of existent vegetated dunes. SET-2 is represented by a U-shaped mound of sand with a convex head trailed by elongated arms with superimposed parabolic dunes (Fig. 1). Wolfe and David (1997) associated this dune configuration to the occurrence of successive episodes of aeolian activity. Maximum dune thickness within SET-2 was around 12 m. Dune geometry is partially vanished inland, while internally subunits are more frequent as a consequence of the occurrence of superimposed dunes.

The internal architecture of the analyzed dunes documents a unique radar unit (U4) with reflections dipping landward in the west–east GPR lines. So far, we have not evidences proving that U4 (SET-2) and U1 (SET-1) are the same unit. The lines oriented north–south presented diverse internal configurations with sub-horizontal reflections and oblique clinoforms oriented both to the north and to the south. An iron crust-like layer, super-surface H3, fossilizes SET-2 (Fig. 4). Sediments within this set are characterized by orange to reddish colors related to iron oxide coatings on the sands.

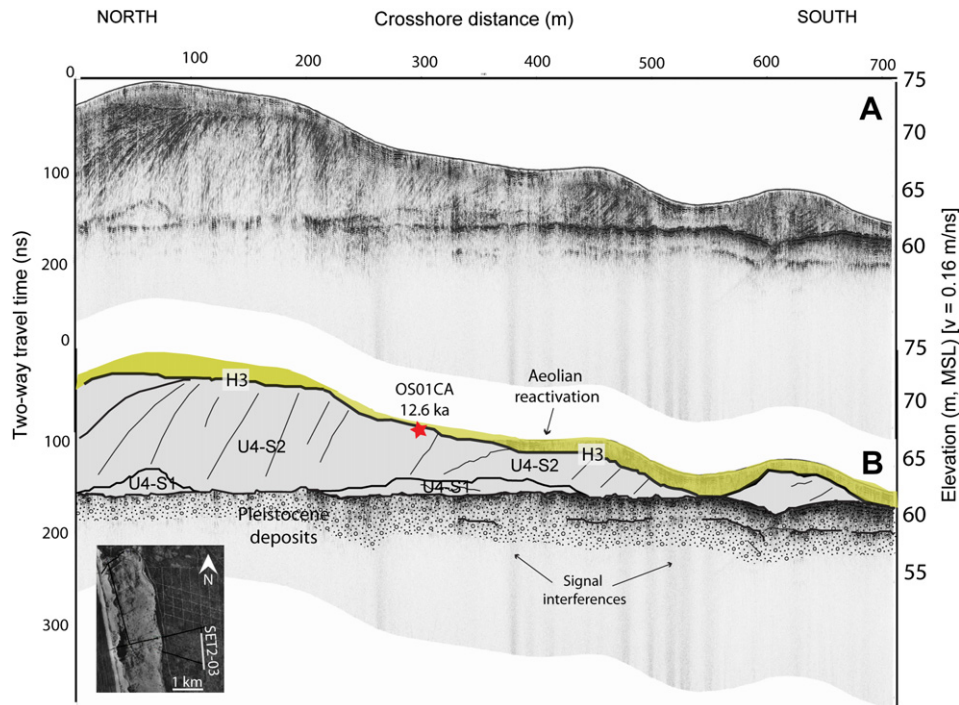


**Fig. 4.** (A) North–south directed GPR profile SET2-03. (B) Interpretation of the radargram with the identified radar units. The location of the sediment sample for dating the radar units is also pointed as well as the resulting ages. Signal interferences were generated by the RTK-GPS system coupled to the GPR.

#### 4.2. Dune chronology

The details of the luminescence age determinations for the studied dunefield are shown in Table 1 and Figs. 1 to 4. OSL ages are presented in thousands of years (ka) before the sampling that took place in 2010. The support of geophysical methods on the decision of sample collection guaranteed the dating of the preserved units representing major episodes of aeolian activity. The OSL ages of the selected radar units range from  $12.6 \pm 0.6$  ka to  $0.30 \pm 0.02$  ka suggesting that the coastal dunefield in the Setúbal peninsula extends from the end of the Pleistocene to the Late-Holocene.

Ages in SET-1 range from  $5.57 \pm 0.21$  ka (radar Unit-2) to  $0.30 \pm 0.02$  ka (radar Unit-3). The lower unit yielding an age of  $5.57 \pm 0.21$  ka can be correlated to the Mid-Holocene climatic reversal at 5.6–5.0 ka documented in the Iberian Peninsula (Carrión, 2002). The westward part of Unit-3 is represented by subunit U3-S1. Samples collected within U3-S1 yielded ages between  $1.22 \pm 0.05$  and  $0.98 \pm 0.05$  ka, correlating to the end of the Dark Ages Cooling event. The younger subunits dated within U3 (U3-S2 and U3-S3) yielded ages between  $0.44 \pm 0.02$  and  $0.30 \pm 0.02$  ka, i.e. both falling well within the time-span of the LIA cooling event. A dune crest in SET-2 yielded an age of  $12.6 \pm 0.6$  ka. In this case, the age of a single dune will be assumed to represent the age of SET-2 despite that they are superimposed parabolic dunes and they are expected to represent successive phases of dune activity. Therefore, the older dunes of the analyzed system fall at the Younger Dryas (YD) cooling event centered in this region at 12 ka (Bard et al., 2000).

#### 4.3. Simulated wind regimes

The results depict the impact of the inter-annual variability of the NAO pattern on near surface (10 m) windfield (Fig. 5). Upper panels in Fig. 5 show the windfield regimes obtained from the reanalysis and analysis data described above at lower resolution

over the wider North-Atlantic and European (NAE) sector, including the impact of the NAO on mean sea-level pressure. Bottom panels zoom in over the target region using the high-resolution hind-casted database (Fig. 5).

During winter months the prevailing winds over the NAE region (between Azores and northern Europe) blow from the southwest, albeit with a stronger intensity for NAO+ than for NAO– (particularly over the UK and northern Europe). In this regard, the intensification of either NAO phases could be compatible with dune building episodes at these latitudes. However, a different picture arises closer to the western Iberian coast where northerly winds dominate the windfield regime during NAO+ and neutral class winters (Fig. 5A and C). This northerly wind configuration is nearly parallel to the orientation of the cliff-top dune crest (Fig. 1). On the contrary, winters characterized as NAO– present a clear westerly component, blowing on the direction of migration of the analyzed dunes (Fig. 5C).

During summer months the wind blows from the north over the Portuguese coast regardless of the NAO phase. Alternatively, the westerly winds intensify during NAO– configuration at northern latitudes, in particular across the French coast (Fig. 5B).

#### 5. Pulses of aeolian activity

The internal architecture of the analyzed dunes as well as their morphology suggest that the transgressive dunefield results from the inland migration of dunes during different pulses of aeolian activity (Fig. 6). The transgressive dunefield is located on top of an elevated terrace located around 50 m above MSL. Considering the different hypothesis suggested for the formation of cliff-top dunes (Haslett et al., 2000) and the internal architecture of the studied dunefield, we propose a three-step mechanism to explain the formation of every pulse of sand accumulation in the study area: (1) in a first stage, transgressive dunes would evolve following an instability in the coastal system induced by a relative fluctuation

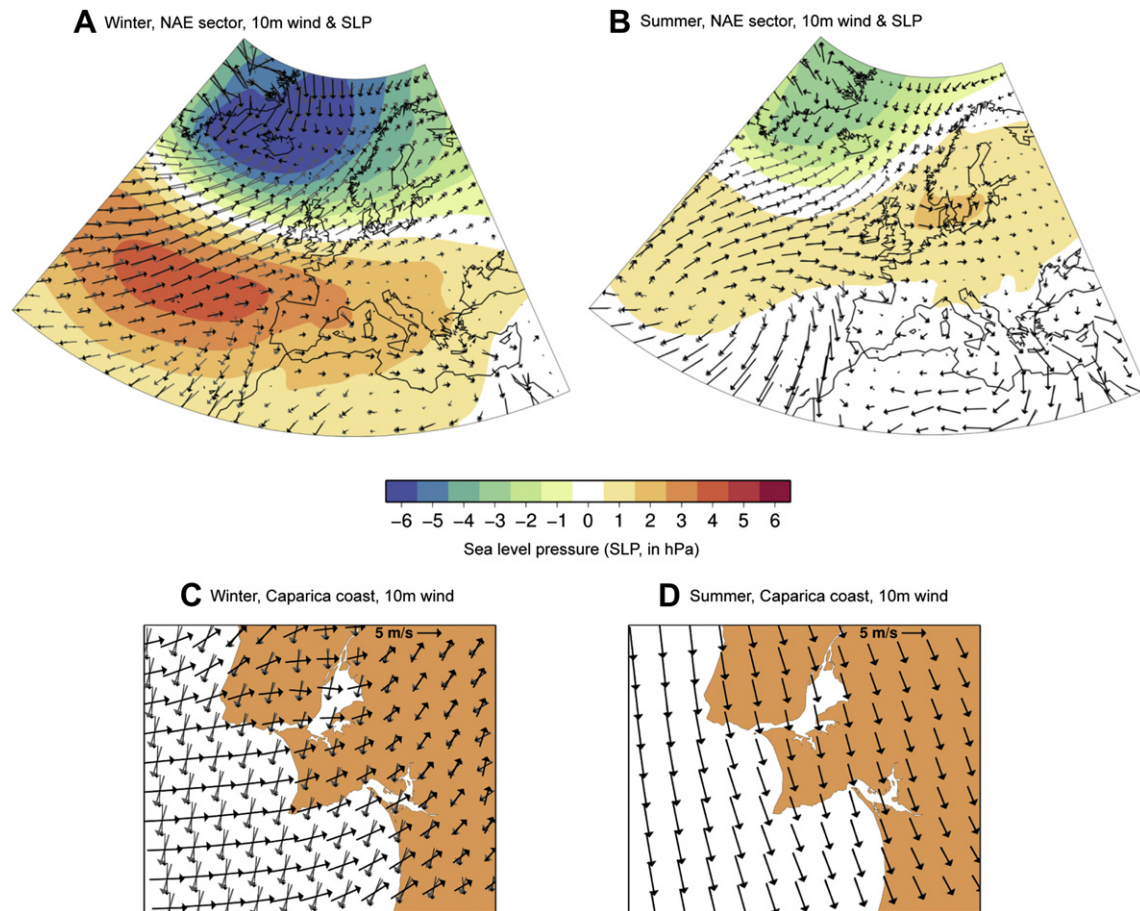


**Fig. 5.** The impact of NAO on 10 m wind direction and module (the length of the arrows is proportional to the wind module) for winter (October-to-March months; left) and summer (June-to-August months; right). Top panels were obtained from the ERA-40 reanalysis and ECMWF analysis data, and depict, for the NAE sector, the mean 10 m windfield during NAO- (black arrows) and NAO+ (gray arrows) phases, and the difference in mean sea-level pressure (SLP) between NAO+ and NAO- phases (NAO+ minus NAO-) by shaded colors (units: hPa). Similarly, bottom panels show the mean 10 m windfield during NAO- (black thick arrows), NAO+ (gray arrows) and normal NAO (black thin arrows) phases at a high-resolution over the Caparica coast. They were obtained from the MM5 simulated data. The averaged period is 1959–2007 in all cases. (For interpretation of the references to colour in this figure legend, the reader is referred to the web version of this article.)

in sea-level and/or enhanced storminess. Psuty (2004) proposed a conceptual model based on the relationship between the sediment budget of the beach and the foredune to explain the formation of transgressive coastal dunes. According to this model, the inland transfer of sand is maximized when the sediment budget is stable or with a minor negative sediment budget. (2) Once transgressive dunes are formed they migrate inland over the antecedent topography (semiconsolidated Pleistocene sediments). Eventually, they could build a sand ramp at the base of the cliff to continue their migration as climbing dunes. Finally, (3) climbing dunes become cliff-top dunes once they reach the edge of the cliff where they can stay fixed or continue its inland migration before being fixed. This mechanism assumes the occurrence of three necessary conditions for the development of every pulse, namely: (i) a seaward location of the shoreline relative to the present position to accommodate the hypothesized aeolian ramp (Ferraz et al., 2011), (ii) elevated sediment supply, and (iii) strong and persistent onshore winds.

The location of the shoreline is controlled by the position of the sea-level and the antecedent topography. In this regard, the relative position of the shoreline may have migrated inland in pace with the deglacial history of sea-level rise. Sediments in the study area are very likely derived from a local source. Here, we hypothesized that the major source of sediment is related to the reworking and recycling of unconsolidated Pleistocene deposits during marine

transgression. A detailed analysis of the sediments within the estuarine beaches of the Tagus estuary (Fig. 1) concluded that the major source of sediments to the beaches derived from the recycling of Pleistocene deposits (Freire et al., 2007).

The last required condition is related to the onset of strong onshore winds, and thus related to the occurrence of appropriate climatic conditions. Current climatic conditions are dominated by the extension and location of the Azores anticyclone during most of the year (Trigo and DaCamara, 2000), which in turn explains the persistence of winds blowing from the north and northwest. The simulations of the atmospheric circulation presented in this work reveal favorable conditions during NAO- winters, when the wind regime along southwestern Europe is clearly dominated by intense westerlies and the storm track is shifted southward. Consequently, we may expect a much higher probability of sustaining the three-step conceptual model during prolonged periods of NAO- like winters.

### 5.1. The onset of the aeolian dunefield

The older aeolian deposits represent the onset of the dunefield extending up to 6 km inland from the present coastline. The first pulse of accumulation constitutes an extended coversand with variable thickness directly overlying the semiconsolidated Pleistocene deposits (Figs. 1 and 4). The only date within the coversand framed its formation at 12.6 ka, when MSL was around 60 m below

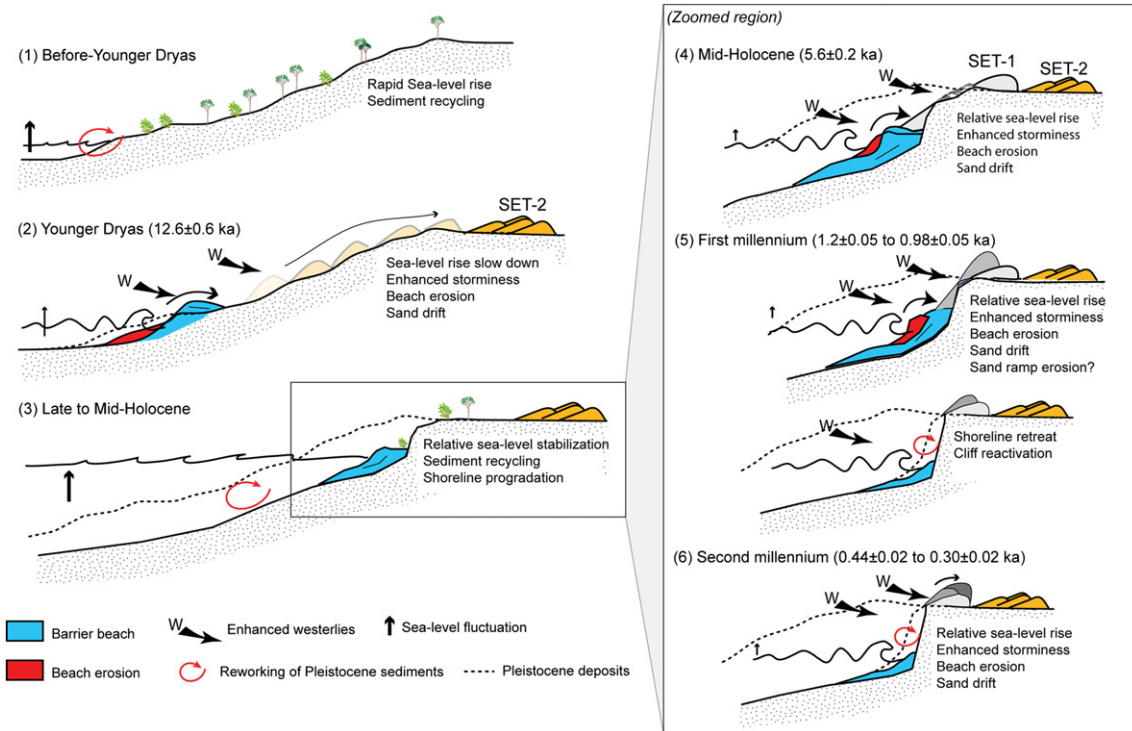


Fig. 6. Proposed coastal evolution of Caparica showing the onset of every pulse of aeolian activity.

present and its rise rate was substantially attenuated (Bard et al., 2010). Sea-level rise attenuation could induce temporary shoreline stabilization and the subsequent incorporation of large volumes of sediment to an incipient coastal barrier through the reworking of Pleistocene deposits (Fig. 6). In this case, the forming transgressive dunes would migrate around 10 km inland from 60 m below present MSL to around 50 m above MSL (Fig. 6). Following this phase of aeolian activity, the transgressive dune stabilized and was subsequently fossilized by a major super-surface with an iron crust-like layer; super-surface H2 (Fig. 4). The formation of this layer could be contemporary to super-surfaces identified in southern Spain (Zazo et al., 2005) or in northern Portugal (Granja et al., 2008) separating dunes active during the YD from those active in the Mid-Holocene. The super-surfaces were related to the onset of moister and temperate climate conditions, which in turn are favorable conditions for dune fixation.

A generalized phase of aeolian activity propagated through western Europe during the YD and Early Holocene. The periglacial aeolian sand-sheet belt, initiated between 28 and 18 ka cal BP in northwest Europe (Kasse, 2002), was reactivated during this period consequence of the strong W–SW winds over northwest Europe (Isarin et al., 1997). This cold climate event also triggered the accumulation of sand dunes in France (Bertran et al., 2009), center (Bateman and Díez Herrero, 2001; García-Hidalgo et al., 2007) and southern Spain (Zazo et al., 2005) and in Portugal (Prudêncio et al., 2007; Bicho et al., 2011). The analysis of the internal architecture of a semiconsolidated dune deposited during this period in central Portugal documented averaged true dips around 22–42° bearing N104°E (Moniz, 1992). This result is compatible with the referred onshore winds responsible for the sedimentation of the cliff-top dunes. However, it significantly differs from the resultant direction of sand transport estimated for present conditions directed N161°E (Rebêlo, 1998).

The YD millennial-duration cold period punctuated the termination of the last glacial period 12.9–11.7 ka ago. Evidences point to

an abrupt strengthening of the westerly winds in western Europe caused by a stronger and more zonal gradient of the North Atlantic sea surface temperature concomitant with the formation of an extensive winter sea-ice cover (Brauer et al., 2008). In the Iberian Peninsula, this period corresponds to an expansion of pioneer species, grasses and semi-desert associations at the expenses of the temperate forest suggesting colder temperatures and increased aridity in the continent (Allen et al., 1996; Carrión, 2002; Gil García et al., 2002; Naughton et al., 2007; Bicho et al., 2011).

## 5.2. Aeolian activity during the Mid-Holocene

Following dune stabilization, a series of dramatic changes altered the configuration of the coast. Sea-level rose from 60 m below present MSL in the YD (Bard et al., 2010) to few meters below present at 7.0 cal yr BP (Vis et al., 2010) forcing the shoreline to migrate inland. Shoreline transgression would induce the erosion of the Pleistocene cover and the subsequent (i) formation of an active retreating cliff, and (ii) the recycling of the Pleistocene sediment into the incipient coastal system. The new configuration of the coast could end with the installation of a prograding coastal barrier simultaneous to most of barriers along the Portuguese coast (Freitas et al., 2003).

A new phase of dune building led to the repetition of the three-step mechanism and the subsequent preservation of the underlying unit within the cliff-top dune ridge (Figs. 1 and 3). The onset of a new phase of aeolian activity could be triggered by a relative instability in the coastline caused by enhanced storminess and/or a sea-level fluctuation. The reactivation of the transgressive dune-field in the toe of the cliff would build a sand ramp and induce the accumulation of a new cliff-top dune at 5.6 ka (Figs. 1, 3 and 6). The end of this phase of aeolian activity is marked by the formation of a new super-surface (H1) with signals of sub-aerial exposure.

Accommodation space and sediment supply were maximized following sea-level stabilization creating favorable conditions for

dune formation along western Europe; i.e. northern Portugal (Granja et al., 2008), south of Spain (Zazo et al., 2005), France (Tastet and Pontee, 1998), United Kingdom (Bateman and Godby, 2004) or Ireland (Wilson et al., 2004). The concordance of these episodes suggests a common driving factor behind the aeolian activity in different latitudes in western Europe following sea-level rise attenuation, which appears intimately linked to climate as it controls wind direction, velocities and distribution.

In the Northern Hemisphere, the period spanning between 6000 and 5000 cal yr BP is characterized by the occurrence of a globally distributed event of rapid climate change (Mayewski et al., 2004) coincident with a major Ice-Rafted Debris (IRD) deposition event taking place at ca 5530 cal yr BP (Bond et al., 2001) (Fig. 7). The suggested potential forcing is the orbitally induced change in insolation enhanced by a non-linear reaction of the climate system. The climate during this period was characterized by cool poles, dry tropics intensified westerlies (Mayewski et al., 2004), and the advance of glaciers in several parts of the world (Grove, 2004; Magny and Haas, 2004). Climate reconstructions of the western Mediterranean region and southern Atlantic coast of Iberia point to a shift towards drier conditions by 6000–4000 (Fletcher et al., 2007; Rodrigo-Gámiz et al., 2011), which tentatively coincides with the onset of an arid episode in northwest Africa (deMenocal et al., 2000; Gasse, 2002). This shift was related to the progressive southward shift of the Northern Hemisphere summer position and likely to a strong tendency towards positive values of the NAO (Wanner et al., 2008) as well as the southward migration of the Intertropical Convergence Zone (ITCZ) (Hodell et al., 2001).

### 5.3. Aeolian activity during the first millennium

The sand unit deposited during this phase of aeolian activity extends landward of the edge of the cliff burying the super-surface H1 (Figs. 1–3). This new pulse of aeolian activity extended at least since 1.2 ka ago (810 AD) to 0.98 ka (970 AD). Sand drift would be firstly triggered by a relative instability of the beach sediment budget probably related to enhanced storminess and/or relative sea-level rise. Coastal instability could eventually force the shoreline to retreat and reactivate the cliff (Fig. 6). As in the previous phases, enhanced and more frequent onshore winds are required to explain the inland transference of aeolian sand.

Simultaneous phases of aeolian activity have been documented in different regions along western Europe such as in England (Wilson et al., 2001; Bateman and Godby, 2004), France (Clarke et al., 2002; Bertran et al., 2011) or northern Portugal (Clarke and Rendell, 2006).

Mayewski et al. (2004) documented a relatively weak climate change event characterized by cool poles and dry tropics occurring 1.2–1.0 ka cal, which coincides with the IRD event taking place at 1.4 ka BP (Bond et al., 2001) (Fig. 7). This phase of aeolian activity

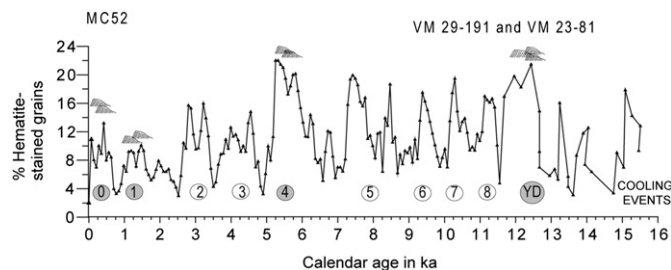


Fig. 7. Correspondence between the pulses of aeolian activity identified in the Caparica dunefield (shadow areas and small dunes) and periods of Northern Hemisphere cooling defined by Bond et al. (1997).

can be tentatively related to the transition between two well-documented global scale climatic events, namely the Dark Ages Cold Event (Keigwin and Pickart, 1999) and the Mediaeval Climatic Anomaly (Diaz et al., 2011). In the Iberian Peninsula this event represents the transition from a period with relatively low fluvial activity to a period with frequent river floods (Carrión, 2002; Benito et al., 2008; Vis et al., 2010). Lower temperatures and drier conditions were also documented in the Iberian Peninsula spanning 270 to 900 AD (Gil García et al., 2007; Martín-Chivelet et al., 2011).

### 5.4. Aeolian activity during the second millennium

The last phase of aeolian sand activity was recorded in the landward part of the cliff-top dune ridge and documents its landward migration. This phase is represented by two subunits documenting the occurrence of two pulses of dune building separated by a superimposition surface dipping landward (Figs. 1 and 2). The results suggest that both pulses are separated by a lapse of time of a hundred years, between 0.44 and 0.35 ka (1560 and 1661 AD). This new pulse contributed to the landward displacement of the dune ridge through the reactivation of the sand unit accumulated during the first millennium (previous pulse). If so, this new pulse would evolve apart from the former shoreline. Shoreline and cliff-top dunes evolved independently following the erosion of the sand ramp, which in turn interrupted the sediment bypass from the shore to the top of the cliff.

A generalized phase of aeolian activity appears to distinguish this time period not only in the Portuguese coast (Clarke and Rendell, 2006), but also in western Europe (Wilson et al., 2001; Clarke et al., 2002; Bateman and Godby, 2004; Björck and Clemmensen, 2004; Aagaard et al., 2007; de Jong et al., 2007; Clarke and Rendell, 2009; Clemmensen et al., 2009). Most of the examples coincide on attributing dune development to enhanced storminess during the LIA.

The LIA was a period of cooling for the North-Atlantic-European region spanning the period between 1550 AD and 1850 AD (Bradley and Jonest, 1993). The LIA was the most recent of the series of cold pulses associated to the accumulation of ice-rafted debris in northern Atlantic sediments (Bond et al., 1997) (Fig. 7). Several mechanisms have been proposed as possible responsible for the occurrence of such a cold pulse (LIA) after the Medieval Climatic Anomaly (Diaz et al., 2011). Among these mechanisms the most widely accepted correspond to changes of external forcing factors, such as changes in solar output or volcanism (Shindell et al., 2001) but also internal variability of the coupled ocean-atmosphere system, e.g. North Atlantic Oscillation (Trouet et al., 2009). Reconstructions of the sea-level pressure (SLP) fields back to 1500 AD indicate persistent negative phase of the NAO during extreme cold periods of the LIA (Luterbacher et al., 2002). These circumstances would have led to reduced influence of the moist and warm zonal flow from the northeastern North Atlantic, yet enhanced precipitation and winds south of 45°N (Raible et al., 2007). However, this simple framework requires some further analysis to explain the occurrence of aeolian activity linked to enhanced storminess across temperate and high latitude North Atlantic. Enhanced storminess during the LIA supported by the ice core, coastal proxies and archival data may be a product of more intense, rather than more frequent storms related to the breakdown of blocking anticyclones (Trouet et al., 2012). On the other hand, instrumental data from meteorological stations in northern Scotland and western Ireland documented periods of exceptional storminess not always coincident with NAO positive phases (Dawson et al., 2002). In turn, they found periods of enhanced storminess coincident with the southward displacement of the polar atmospheric, the oceanographic front and a marked southward displacement in of the North Atlantic storm track.

The sedimentary record from the continental shelf off Portugal suggests enhanced continental influence by river runoff (Abrantes et al., 2005; Gil et al., 2006). The authors interpreted these results as indicative of persistent negative phases of the NAO or frequent extreme NAO minima events (Abrantes et al., 2005, 2011). In fact, according to several paleo-hydrological studies the LIA period corresponded to a wetter than usual period in Iberia, with frequent flooding events (Benito et al., 2008; Sousa and García-Murillo, 2003). Nevertheless, according to other authors, the LIA was experienced as a series of frequent fluctuations rather than a uniform period (Alcoforado et al., 2000; Domínguez-Castro et al., 2010; Machado et al., 2011).

The first pulse of aeolian activity documented here and dated at 0.44 ka (1570 AD) could be tentatively related to the onset of the LIA or to the transition towards an extremely cold episode within the LIA, the Maunder Minimum (1640–1715). The second pulse of dune building dated at 0.3 ka ago (1710 AD) is coincident with the end of the Maunder Minimum cold event. These results suggest that the pulses of aeolian activity during the LIA were coincident with changing climate conditions within a specific cold event. Whether the accumulation of aeolian sand corresponded to drier or moister periods at a regional scale is a complex problem considering the limitations on the understanding the climate variability in the region and the reduced number of dated samples. However, both episodes of aeolian activity can tentatively be correlated with continuous decadal wet and flood events identified by Machado et al. (2011).

### 5.5. Environmental implications

The record of aeolian activity in Caparica suggests that the Portuguese coast was intermittently inundated by aeolian sands at least since the termination of the last glacial period. The accumulation of large transgressive coastal dunes, dated at 12.6, 5.6, 1.2, 0.44 and 0.3 ka ago, alternated with phases of dune stabilization recorded as super-surfaces and superimposition surfaces. These results envision a scenario completely different from what we see today, represented by sediment saturated coastal systems and large transgressive dunefields. Here we propose a mechanism whereby this scenario results from the reworking of older deposits (Pleistocene) during the marine transgression and the onset of intense westerly winds dominating the windfield.

A central question on coastal dune development has been whether periods of sand drift record storm incidence, climate change, sea-level or a combination of them (Long, 2003). The temporal correspondence between cold climate events with global distribution and the pulses of aeolian activity in Portugal suggests a strong climate control. The mentioned cold events involved the co-occurrence of North Atlantic cooling, advance of the sea-ice cover southward forcing the North Atlantic storm track to displace in the same direction, and enhanced storminess in the North Atlantic. Regionally, the manifestation of cold events changed over time, with significant differences regarding the average temperatures or aridity. However, our results reflect a windfield clearly dominated by intense westerlies during all the identified episodes of dune building. In addition, it has been reported here that the phases of aeolian activity in Caparica are coeval with well-documented episodes of dune accumulation in western Europe. Correspondence between dune accumulation in NW Europe and Central Spain has been previously reported for the YD cold event (Bateman and Díez Herrero, 2001). However, Clarke and Rendell (2006) found that during more recent times, dune building in France (AD 1452–1752) and Portugal (AD 1770–1905) were markedly asynchronous. The authors associated this difference to changes in the Atlantic storm tracks driven by changes in the predominant phase of the NAO pattern. Contrary to the results

from Clarke and Rendell (2006), our results support the hypothesized simultaneous aeolian activity along the western coast of Europe as we found that the aeolian activity in Caparica (Portugal) and France during the LIA were simultaneous.

Aeolian activity in western Europe has been related to changing climate conditions (Clemmensen et al., 2001; Bateman and Godby, 2004; de Jong et al., 2007), in particular to enhanced storminess (Clarke and Rendell, 2009). However, the actual mechanism through which storminess enhances aeolian activity remains unsolved. A possible mechanism bases the inland transference of sand on the constructive action of single events such as storm surges (Regnaud et al., 2004; Aagaard et al., 2007). Storminess may also induce coastal erosion and strong wind reworking of beach and foredune sediments (Clemmensen et al., 2001), or increase the number of days when wind velocities have the capability of moving sand (Bateman and Godby, 2004). In this regard, recent research in coastal and inland dunes suggest that aeolian activity is primarily the result of wind power, and as such, even in humid climates exposed dunes can be mobilized (Tsoar et al., 2009; Roskin et al., 2011).

Our results suggest that pulses of aeolian activity in Caparica were initiated by coastal instabilities and driven by intense westerlies in a context of sea-level rise. Evidences suggest significant accelerations in the rate of sea-level rise before Mid-Holocene due to ice sheet retreat (Bard et al., 2010; Bird et al., 2010). From 7 ka until present, the volume of mass transfer between ice sheets and oceans was apparently no more than  $\pm 1$  m (eustatic sea-level equivalent) (Milne et al., 2005). Yet, local fluctuations in relative sea-level (less than 1 m) driven primarily by winds or currents during the Late-Holocene may have had significant impact on coastlines (Goy et al., 2003). Such fluctuations could contribute to coastal instability enhancing the negative effect of storms on the coastal sediment budget and to sand drift initiation.

The temporal concordance between phases of aeolian activity in the North-Atlantic-European coast and the South Atlantic European coast, between 55 and 36°N, suggests intense and frequent westerlies crossing the North Atlantic in a more zonal flow. In this line, mesoscale and regional simulations presented here envision a possible scenario of atmospheric circulation to explain intense and frequent westerlies crossing the North Atlantic. These results suggest aeolian accumulation along northwestern Europe compatible with prolonged periods of NAO– during summer months (Fig. 5), albeit it could be compatible with both NAO– and NAO+ in winter. By contrast, the formation of the transgressive dunes in Caparica requires prolonged periods of the NAO– pattern during winter as presented in Section 4.3. These results are indeed compatible with the reconstructions of monthly and seasonal surface temperature fields for Europe back to 1500 (Cook et al., 2002; Luterbacher et al., 2004). In addition, NAO paleo-reconstructions show a certain agreement with such an hypothesis. For example, it is documented that negative phases of NAO prevailed during most of the phases of aeolian accumulation identified in Caparica, namely during the phases dated at 5.6 ka (Mid-Holocene) and at 0.44 and 0.3 ka (LIA). Moreover, Trouet et al. (2009) suggested a sustained NAO+ during MCA, and Wannert et al. (2008) reported a change from NAO– in the Middle Holocene to NAO+ during the Late-Holocene (with NAO+ prevailing afterwards); both periods coinciding with phases of dune stabilization. However, we must acknowledge that the NAO pattern may have changed throughout the Holocene. In fact, several works have shown that the NAO pattern, and associated climatic impacts, can vary at the decadal (Trigo et al., 2004) and centennial (Pauling et al., 2006) time scales. Nevertheless, these changes are often related with the recent accessibility to vast amounts of climatic data allowing the assessment of the NAO impact at very high-resolution. Moreover, despite the mentioned changes, the overall aspect of the

NAO pattern has remained very similar since the early 1800s, particularly at the relevant scales for this work (Vicente-Serrano and López-Moreno, 2008).

Further research on the present dunefield is needed to improve the temporal resolution of the identified phases of aeolian activity or to confirm the occurrence of aeolian activity during other cold climatic events. Despite the larger number of cold climate episodes affecting the north Atlantic basin since the glacial termination, we have identified only four phases of aeolian activity meaning that (1) only during those events the conditions were favorable for dune accumulation, or (2) more phases of dune activity could occur, yet these were not sampled or not preserved within the aeolian record. On the other hand, it is worthy to mention that not all dunes in the Portuguese coast were driven by enhanced westerlies. Transgressive dunefields driven by northerly winds were identified 18 km to the south of the present study area burying roman ruins (Rebêlo et al., 2009) suggesting the onset of contrasting environmental conditions relative to the westerly driven dunes.

## 6. Conclusions

The climate is thought to be responsible for the formation of aeolian deposits. In northwest Europe, significant phases of aeolian activity have been related to periods of enhanced storminess. However, the spatial and temporal extent of these events remains poorly understood. We address this question by analyzing the aeolian record of Caparica in Portugal. The widespread presence of stabilized transgressive dunefields across the Portuguese coast provides an excellent opportunity to investigate the climate of the past in southwest Europe.

The cliff-top transgressive dunefield from Caparica documents several pulses of aeolian activity separated by periods of dune stabilization. It has been hypothesized that these dunes are part of a major transgressive dunefield genetically linked to a former shoreline, which provided the sediment to the dunes. This hypothesis assumes: (i) a seaward location of the shoreline relative to its present position, (ii) enhanced sediment supply, and (iii) strong and persistent westerly windfield, which contrasts with the pattern of atmospheric circulation in the present-day. Every pulse of aeolian activity was hypothesized to be preceded by instability in the shoreline exposing large volumes of sediment to the effect of intensified onshore winds. If so, aeolian activity was apparently initiated by coastal instability, which in turn could be triggered by a positive fluctuation of relative sea-level superposed to the effect of enhanced storminess.

The aeolian record extends since the termination of the last glacial to historical times with pulses at 12.6, 5.6, 1.2, 0.44 and 0.3 ka ago. Pulses of aeolian activity were tentatively correlated to cold climate events of global distribution and other pulses of aeolian activity along Western Europe. The correspondence between cold climate events and aeolian activity suggests that cooling events were responsible for the intensification of westerlies across the North Atlantic. Model simulations based on current modes of atmospheric variability provided a possible scenario compatible with the accumulation of aeolian sands in the past. Phases of aeolian activity across Portugal and NW Europe could occur during prolonged negative phases of the NAO that would explain the enhancement of westerly winds across Portugal during winter and across NW Europe during summer months.

## Acknowledgments

This research was funded by the Portuguese Science Foundation (FCT) through the projects SCARPS (PTDC/CTE-GIX/101466/2008) and ENAC (PTDC/AAC-CLI/103567/2008). Susana Costas

thanks the FCT for financial support through the program Ciência-2007. Sonia Jerez received a scholarship from FCT within the framework of project ENAC. Special thanks are given to Gabriel Menezes, Pedro Brito and Marco Ferraz for their help with field work. We would like also to acknowledge the MAR research group from of the University of Murcia for providing results from the MM5 high-resolution atmospheric simulation. Thanks to Seismic Micro-Technology Inc. who kindly provided a license of Kingdom Suite software to the University of Vigo.

## References

- Aagaard, T., Orford, J., Murray, A.S., 2007. Environmental controls on coastal dune formation; Skallingen Spit, Denmark. *Geomorphology* 83, 29–47.
- Abrantes, F., Lebreiro, S., Rodrigues, T., Gil, I., Bartels-Jónsdóttir, H., Oliveira, P., Kissel, C., Grimalt, J.O., 2005. Shallow-marine sediment cores record climate variability and earthquake activity off Lisbon (Portugal) for the last 2000 years. *Quaternary Science Reviews* 24, 2477–2494.
- Abrantes, F., Rodrigues, T., Montanari, B., Santos, C., Witt, L., Lopes, C., Voelker, A.H.L., 2011. Climate of the last millennium at the southern-pole of the North Atlantic Oscillation: an inner-shelf sediment record of flooding and upwelling. *Climate Research* 48, 261–280.
- Adamic, G., Aitken, M., 1998. Dose-rate conversion factors: update. *Ancient TL* 16, 37–50.
- Aitken, M.J., 1998. *An Introduction to Optical Dating. The Dating of Quaternary Sediments by the Use of Photon-stimulated Luminescence* Oxford University Press.
- Alcoforado, M.-J., Nunes, M.d.F., Garcia, J.C., Taborda, J.P., 2000. Temperature and precipitation reconstruction in southern Portugal during the late Maunder Minimum (AD 1675–1715). *The Holocene* 10, 333–340.
- Alcoforado, M.J., 1992. *O Clima da Região de Lisboa*. Centro de Estudos Geográficos da Universidade de Lisboa, Lisbon.
- Allen, J.R.M., Huntley, B., Watts, W.A., 1996. The vegetation and climate of northwest Iberia over the last 14,000 years. *Journal of Quaternary Science* 11, 125–147.
- Andrade, C., Freitas, C., Cachado, C., Cardoso, A.C., Monteiro, J.H., Brito, P., Rebelo, L., 2002. Coastal zones. In: Santos, F.D., Forbes, K., Moita, R. (Eds.), *Climate Change in Portugal. Scenarios, Impacts and Adaptation Measures SIAM project*, Gradiva, Lisboa, pp. 173–219.
- Antunes, M.T., Pais, J., 1989. Paisagem protegida da Arriba Fossil da Caparica. Centro de estratigrafia e paleobiologia da U.N.L. (I.N.I.C.).
- Azevedo, M.T., 1983. O sinclinal de Albufeira, Evolução pós miocénica e reconstrução paleogeográfica. Universidade de Lisboa, Lisboa, 302 p.
- Bailey, R.M., Arnold, L.J., 2006. Statistical modeling of single grain quartz  $D_e$  distributions and an assessment of procedures for estimating burial dose. *Quaternary Science Reviews* 25, 2475–2502.
- Bard, E., Rostek, F., Turon, J.-L., Gendreau, S., 2000. Hydrological impact of Heinrich events in the subtropical northeast Atlantic. *Science* 289, 1321–1324.
- Bard, E., Hamelin, B., Delanghe-Sabatier, D., 2010. Deglacial meltwater pulse 1B and Younger Dryas Sea levels revisited with Boreholes at Tahiti. *Science* 327, 1235–1237.
- Bateman, M.D., Díez Herrero, A., 2001. The timing and relation of aeolian sand deposition in central Spain to the aeolian sand record of NW Europe. *Quaternary Science Reviews* 20, 779–782.
- Bateman, M.D., Godby, S.P., 2004. Late-Holocene inland dune activity in the UK: a case study from Breckland, East Anglia. *The Holocene* 14, 579–588.
- Bateman, M.D., 1995. Thermoluminescence dating of the British coversand deposits. *Quaternary Science Reviews* 14, 791–798.
- Benito, G., Thorndycraft, V.R., Rico, M., Sánchez-Moya, Y., Sopena, A., 2008. Palaeoflood and floodplain records from Spain: evidence for long-term climate variability and environmental changes. *Geomorphology* 101, 68–77.
- Bertran, P., Allenet, G., Gé, T., Naughton, F., Poirier, P., Goñi, M.F.S., 2009. Coversand and Pleistocene palaeosols in the Landes region, southwestern France. *Journal of Quaternary Science* 24, 259–269.
- Bertran, P., Bateman, M.D., Hernandez, M., Mercier, N., Millet, D., Sitzia, L., Tastet, J.-P., 2011. Inland aeolian deposits of south-west France: facies, stratigraphy and chronology. *Journal of Quaternary Science* 26, 374–388.
- Bicho, N., Haws, J., Almeida, F., 2011. Hunter-gatherer adaptations and the Younger Dryas in central and southern Portugal. *Quaternary International* 242, 336–347.
- Bird, M.I., Austin, W.E.N., Wurster, C.M., Fifield, L.K., Mojtabid, M., Sargeant, C., 2010. Punctuated eustatic sea-level rise in the early Mid-Holocene. *Geology* 38, 803–806.
- Björck, S., Clemmensen, L.B., 2004. Aeolian sediment in raised bog deposits, Halland, SW Sweden: a new proxy record of Holocene winter storminess variation in southern Scandinavia? *The Holocene* 14, 677–688.
- Bond, G., Showers, W., Cheseby, M., Lotti, R., Almasi, P., deMenocal, P., Priore, P., Cullen, H., Hajdas, I., Bonani, G., 1997. A pervasive millennial-scale cycle in North Atlantic Holocene and Glacial climates. *Science* 278, 1257–1266.
- Bond, G., Kromer, B., Beer, J., Muscheler, R., Evans, M.N., Showers, W., Hoffmann, S., Lotti-Bond, R., Hajdas, I., Bonani, G., 2001. Persistent solar influence on North Atlantic climate during the Holocene. *Science* 294, 2130–2136.
- Bradley, R.S., Jonest, P.D., 1993. 'Little Ice Age' summer temperature variations: their nature and relevance to recent global warming trends. *The Holocene* 3, 367–376.

- Brauer, A., Haug, G.H., Dulski, P., Sigman, D.M., Negendank, J.F.W., 2008. An abrupt wind shift in western Europe at the onset of the Younger Dryas cold period. *Nature Geoscience* 1, 520–523.
- Bristow, C.S., 2009. Ground penetrating radar in aeolian sand dunes. In: Jol, H.M. (Ed.), *Ground Penetrating Radar Theory and Applications*. Elsevier Science, Amsterdam, pp. 273–298.
- Carrión, J.S., 2002. Patterns and processes of Late Quaternary environmental change in a montane region of southwestern Europe. *Quaternary Science Reviews* 21, 2047–2066.
- Clarke, M.L., Rendell, H.M., 2006. Effects of storminess, sand supply and the North Atlantic Oscillation on sand invasion and coastal dune accretion in western Portugal. *The Holocene* 16, 341–355.
- Clarke, M.L., Rendell, H.M., 2009. The impact of North Atlantic storminess on western European coasts: a review. *Quaternary International* 195, 31–41.
- Clarke, M., Rendell, H., Tastet, J.-P., Clave, B., Masse, L., 2002. Late-Holocene sand invasion and North Atlantic storminess along the Aquitaine coast, southwest France. *The Holocene* 12, 231–238.
- Clemmensen, L.B., Pye, K., Murray, A., Heinemeier, J., 2001. Sedimentology, stratigraphy and landscape evolution of a Holocene coastal dune system, Lodbjerg, NW Jutland, Denmark. *Sedimentology* 48, 3–27.
- Clemmensen, L.B., Murray, A., Heinemeier, J., de Jong, R., 2009. The evolution of Holocene coastal dune fields, Jutland, Denmark: a record of climate change over the past 5000 years. *Geomorphology* 105, 303–313.
- Cook, E.R., D'Arrigo, R.D., Mann, M.E., 2002. A well-Verified, Multiproxy reconstruction of the winter North Atlantic oscillation index since A.D. 1400. *Journal of Climate* 15, 1754–1764.
- Costas, S., Brito, P.O., Ferraz, M., González-Villanueva, R., Novo, A., Rebêlo, L., 2010. The cliff-top dune of Costa da Caparica: possible scenarios of formation and evolution. In: Freitas, M.C., Andrade, C. (Eds.), *Coastal Hope 2010*, Lisboa, pp. 27–28.
- Danielsen, R., Castilho, A.M., Dinis, P.A., Almeida, A.C., Callapez, P.M., 2011. Holocene interplay between a dune field and coastal lakes in the Quiaios–Tocha region, central littoral Portugal. *The Holocene*.
- Dawson, A.G., Hickey, K., Holt, T., Elliott, L., Dawson, S., Foster, I.D.L., Wadhams, P., Jonsdottir, I., Wilkinson, J., McKenna, J., Davis, N.R., Smith, D.E., 2002. Complex North Atlantic Oscillation (NAO) index signal of historic North Atlantic storm-track changes. *The Holocene* 12, 363–369.
- de Jong, R., Schoning, K., Björck, S., 2007. Increased aeolian activity during climatic regime shifts as recorded in a raised bog in south-west Sweden during the past 1700 years. *Climate of the Past Discussion* 3, 383–408.
- deMenocal, P., Ortiz, J., Guilderson, T., Adkins, J., Sarnthein, M., Baker, L., Yarusinsky, M., 2000. Abrupt onset and termination of the African Humid Period: rapid climate responses to gradual insolation forcing. *Quaternary Science Reviews* 19, 347–361.
- Diaz, H.F., Trigo, R., Hughes, M.K., Mann, M.E., Xoplaki, E., Barriopedro, D., 2011. Spatial and temporal characteristics of climate in medieval times revisited. *Bulletin of the American Meteorological Society*.
- Domínguez-Castro, F., García-Herrera, R., Ribera, P., Barriendos, M., 2010. A shift in the spatial pattern of Iberian droughts during the 17th century. *Climate of the Past Discussion* 6, 1111–1137.
- Durcan, J.A., Duller, G.A.T., Roberts, H.M., 2009. A Simple Criterion for Identifying Quartz OSL Signals Dominated by the Fast Component, UK Luminescence and ESR Meeting 2009. Royal Holloway of London.
- Eurosion, 2004. Living with Coastal Erosion in Europe: Sediment and Space for Sustainability. In: Part II – Maps and Statistics, 25 p.
- Ferraz, M., Cowell, P., Rebêlo, L., 2011. Coastal-change estimates inferred from remnant cliff-top dunes. *Journal of Coastal Research SI 64* (Proceedings of the 11th International Coastal Symposium), 661–665.
- Fletcher, W.J., Boski, T., Moura, D., 2007. Palynological evidence for environmental and climatic change in the lower Guadiana valley, Portugal, during the last 13 000 years. *The Holocene* 17, 481–494.
- Freire, P., Taborda, R., Silva, A., 2007. Sedimentary characterization of Tagus estuarine beaches (Portugal). *Journal of Soils and Sediments* 7, 296–302.
- Freitas, M.C., Andrade, C., Rocha, F., Tassinari, C., Munhá, J.M., Cruces, A., Vidinha, J., Da Silva, C.M., 2003. Lateglacial and Holocene environmental changes in Portuguese coastal lagoons 1: the sedimentological and geochemical records of the Santo André coastal area. *The Holocene* 13, 433–446.
- Galbraith, R.F., Roberts, R.G., Laslett, G.M., Yoshida, H., Olley, J.M., 1999. Optical dating of single and multiple grains of quartz from Jinmium Rock Shelter, Northern Australia: Part 1, experimental design and statistical models. *Archaeometry* 41, 339–364.
- García-Hidalgo, J.F., Temiño, J., Segura, M., 2007. Holocene aeolian development in Central Spain: chronology, regional correlations and causal processes. *Quaternary Science Reviews* 26, 2661–2673.
- Gasse, F., 2002. Diatom-inferred salinity and carbonate oxygen isotopes in Holocene waterbodies of the western Sahara and Sahel (Africa). *Quaternary Science Reviews* 21, 737–767.
- Gil, I.M., Abrantes, F., Hebbeln, D., 2006. The North Atlantic Oscillation forcing through the last 2000 years: spatial variability as revealed by high-resolution marine diatom records from N and SW Europe. *Marine Micropaleontology* 60, 113–129.
- Gil García, M.J., Valiño, M.D., Rodríguez, A.V., Zapata, M.B.R., 2002. Late-glacial and Holocene palaeoclimatic record from Sierra de Cebollera (northern Iberian Range, Spain). *Quaternary International* 93–94, 13–18.
- Gil García, M., Ruiz Zapata, M., Santisteban, J., Mediavilla, R., López-Pamo, E., Dabrio, C., 2007. Late holocene environments in Las Tablas de Daimiel (south central Iberian peninsula, Spain). *Vegetation History and Archaeobotany* 16, 241–250.
- Giorgi, F., 2006. Climate change hot-spots. *Geophysical Research Letters* 33, L08707.
- Goy, J.L., Zazo, C., Dabrio, C.J., 2003. A beach-ridge progradation complex reflecting periodical sea-level and climate variability during the Holocene (Gulf of Almería, Western Mediterranean). *Geomorphology* 50, 251–268.
- Granja, H.M., Groot, T.A.M.D., Costa, A.L., 2008. Evidence for Pleistocene wet aeolian dune and interdune accumulation, S. Pedro da Maceda, north-west Portugal. *Sedimentology* 55, 1203–1226.
- Grell, G.A., Dudhia, J., Stauffer, D.R., 1995. A description of the fifth-generation Penn State/NCAR Mesoscale Model (MM5). NCAR Tech. Note TN398 STR, 138 pp.
- Grove, J., 2004. *Little Ice Ages: Ancient and Modern*. Routledge, New York.
- Haslett, S.K., Davies, P., Curr, R.H.F., 2000. Geomorphologic and Palaeoenvironmental development of Holocene perched coastal dune systems in Brittany, France. *Geografiska Annaler: Series A, Physical Geography* 82, 79–88.
- Hodell, D.A., Brenner, M., Curtis, J.H., Guilderson, T., 2001. Solar forcing of drought frequency in the Maya Lowlands. *Science* 292, 1367–1370.
- Hughenoltz, C.H., Wolfe, S.A., Moorman, B.J., 2008. Effects of sand supply on the morphodynamics and stratigraphy of active parabolic dunes, Bigstick Sand Hills, southwestern Saskatchewan Geological Survey of Canada Contribution 20060654. *Canadian Journal of Earth Sciences* 45, 321–335.
- Hurrell, J.W., 1995. Decadal trends in the North Atlantic oscillation: regional temperatures and precipitation. *Science* 269, 676–679.
- IPCC, 2007. *Climate change 2007: the physical science basis*. In: Solomon, S., Qin, D., Manning, M., Chen, Z., Marquis, M., Averyt, K.B., Tignor, M., Miller, H.L. (Eds.), *Contribution of Working Group I to the Fourth Assessment Report of the Intergovernmental Panel on Climate Change*. Cambridge, United Kingdom and New York, NY, USA, 996 p.
- Isarin, R.F.B., Renssen, H., Koster, E.A., 1997. Surface wind climate during the Younger Dryas in Europe as inferred from aeolian records and model simulations. *Palaeogeography, Palaeoclimatology, Palaeoecology* 134, 127–148.
- Jones, P.D., Jonsson, T., Wheeler, D., 1997. Extension to the North Atlantic oscillation using early instrumental pressure observations from Gibraltar and south-west Iceland. *International Journal of Climatology* 17, 1433–1450.
- Kasse, C., 1997. Cold-Climate aeolian sand-sheet formation in North-Western Europe (c. 14–12.4 ka); a Response to Permafrost Degradation and increased aridity. *Permafrost and Periglacial Processes* 8, 295–311.
- Kasse, C., 2002. Sandy aeolian deposits and environments and their relation to climate during the Last Glacial Maximum and Lateglacial in northwest and central Europe. *Progress in Physical Geography* 26, 507–532.
- Keigwin, L.D., Pickart, R.S., 1999. Slope water current over the Laurentian Fan on interannual to millennial time scales. *Science* 286, 520–523.
- Kocurek, G., 1991. Interpretation of ancient eolian sand dunes. *Annual Review of Earth and Planetary Sciences* 19, 43–75.
- Long, A., 2003. The coastal strip: sea-level change, coastal evolution and land-ocean correlation. *Progress in Physical Geography* 27, 423–434.
- Lorente-Plazas, R., 2010. *Elaboración de una base de datos pseudoreal para la evaluación del potencial eólico para Minieólica*. MSc Thesis. Universidad de Granada, Spain.
- Luterbacher, J.L., Xoplaki, E.X., Dietrich, D.D., Rickli, R.R., Jacobeit, J.J., Beck, C.B., Gyalistras, D.G., Schmutz, C.S., Wanner, H.W., 2002. Reconstruction of sea level pressure fields over the Eastern North Atlantic and Europe back to 1500. *Climate Dynamics* 18, 545–561.
- Luterbacher, J., Dietrich, D., Xoplaki, E., Grosjean, M., Wanner, H., 2004. European seasonal and annual temperature variability, trends, and extremes since 1500. *Science* 303, 1499–1503.
- Machado, M.J., Benito, G., Barriendos, M., Rodrigo, F.S., 2011. 500 Years of rainfall variability and extreme hydrological events in southeastern Spain drylands. *Journal of Arid Environments* 75, 1244–1253.
- Magny, M., Haas, J.N., 2004. A major widespread climatic change around 5300 cal. yr BP at the time of the Alpine Ice man. *Journal of Quaternary Science* 19, 423–430.
- Martín-Chivelet, J., Muñoz-García, M.B., Edwards, R.L., Turrero, M.J., Ortega, A.I., 2011. Land surface temperature changes in Northern Iberia since 4000 yr BP, based on [delta]13C of speleothems. *Global and Planetary Change* 77, 1–12.
- Mayewski, P.A., Rohling, E.E., Curt Stager, J., Karlén, W., Maasch, K.A., David Meecker, L., Meyerson, E.A., Gasse, F., van Kreveld, S., Holmgren, K., Lee-Thorp, J., Rosqvist, G., Rack, F., Staubwasser, M., Schneider, R.R., Steig, E.J., 2004. Holocene climate variability. *Quaternary Research* 62, 243–255.
- Milne, G.A., Long, A.J., Bassett, S.E., 2005. Modelling Holocene relative sea-level observations from the Caribbean and South America. *Quaternary Science Reviews* 24, 1183–1202.
- Moniz, C., 1992. *Análise de fracturação. Exemplos de aplicação nas dunas consolidadas de Oitavos e Praia da Aguda, Tema das provas de aptidão pedagógica e capacidade científica*. Universidade de Lisboa (F.C.U.L.), Lisbon.
- Murray, A.S., Wintle, A.G., 2000. Luminescence dating of quartz using an improved single-aliquot regenerative-dose protocol. *Radiation Measurements* 32, 57–73.
- Murray, A.S., Wintle, A.G., 2003. The single aliquot regenerative dose protocol: potential for improvements in reliability. *Radiation Measurements* 37, 377–381.
- Naughton, F., Sanchez Goñi, M.F., Desprat, S., Turon, J.L., Duprat, J., Malaizé, B., Joli, C., Cortijo, E., Drago, T., Freitas, M.C., 2007. Present-day and past (last 25 000 years) marine pollen signal off western Iberia. *Marine Micropaleontology* 62, 91–114.

- Pauling, A., Luterbacher, J., Casty, C., Wanner, H., 2006. Five hundred years of gridded high-resolution precipitation reconstructions over Europe and the connection to large-scale circulation. *Climate Dynamics* 26, 387–405.
- Prescott, J.R., Hutton, J.T., 1994. Cosmic ray contributions to dose rates for luminescence and ESR dating: large depths and long-term time variations. *Radiation Measurements* 23, 497–500.
- Prudêncio, M.I., Marques, R., Rebelo, L., Cook, G.T., Cardoso, G.O., Naysmith, P., Freeman, S.P.H.T., Franco, D., Brito, P., Dias, M.I., 2007. Radiocarbon and blue optically stimulated luminescence chronologies of the Oitavos consolidated Dune (Western Portugal). *Radiocarbon* 49, 1145–1151.
- Psuty, N., 2004. The coastal foredune: a morphological basis for regional coastal dune development. In: ML, M., NP, P. (Eds.), *Coastal Dunes, Ecology and Conservation*. Springer-Verlag, Berlin, pp. 11–27.
- Raible, C., Yoshimori, M., Stocker, T., Casty, C., 2007. Extreme midlatitude cyclones and their implications for precipitation and wind speed extremes in simulations of the Maunder Minimum versus present day conditions. *Climate Dynamics* 28, 409–423.
- Ramos Pereira, A., Angelucci, D.E., 2004. Formações dunares no litoral português, do final do Plistocénico e inícios do Holocénico, como indicadores paleoclimáticos e paleogeográficos. In: Tavares, A.A., Ferro Tavares, M.J., Cardoso, J.L. (Eds.), *Evolução geohistórica do litoral português e fenómenos correlativos*. Geologia, História, Arqueologia e Climatologia. Universidade Aberta, pp. 221–256.
- Rebêlo, L.P., Brito, P.O., Monteiro, J.H., 2002. Monitoring the Cresmina dune evolution (Portugal) using differential GPS. *Journal of Coastal Research* SI 36, 591–604.
- Rebêlo, L., Ferraz, M., Brito, P., 2009. Tróia Peninsula evolution: the dune morphology record. *Journal of Coastal Research* SI56, 352–355.
- Rebêlo, L.P., 1998. Dinâmica do sistema dunar do Guincho-Oitavos, V Congresso Nacional de Geologia. Instituto Geológico e Mineiro, Lisboa, C83–C84 pp.
- Regnaud, H., Pirazzoli, P.A., Morvan, G., Ruz, M., 2004. Impacts of storms and evolution of the coastline in western France. *Marine Geology* 210, 325–337.
- Renssen, H., Kasse, C., Vandenberghe, J., Lorenz, S.J., 2007. Weichselian Late Pleniglacial surface winds over northwest and central Europe: a model–data comparison. *Journal of Quaternary Science* 22, 281–293.
- Rodrigo-Gámiz, M., Martínez-Ruiz, F., Jiménez-Espejo, F.J., Gallego-Torres, D., Nieto-Moreno, V., Romero, O., Ariztegui, D., 2011. Impact of climate variability in the western Mediterranean during the last 20,000 years: oceanic and atmospheric responses. *Quaternary Science Reviews* 30, 2018–2034.
- Roskin, J., Tsoar, H., Porat, N., Blumberg, D.G., 2011. Palaeoclimate interpretations of Late Pleistocene vegetated linear dune mobilization episodes: evidence from the northwestern Negev dunefield, Israel. *Quaternary Science Reviews* 30, 3364–3380.
- Schirmer, W., 1999. *Dunes and Fossil Soils*, vol. 3. GeoArchaeoRhein.
- Shindell, D.T., Schmidt, G.A., Mann, M.E., Rind, D., Waple, A., 2001. Solar forcing of regional climate change during the Maunder minimum. *Science* 294, 2149–2152.
- Sousa, A., García-Murillo, P., 2003. Changes in the Wetlands of Andalusia (Doñana Natural Park, SW Spain) at the end of the Little Ice Age. *Climatic Change* 58, 193–217.
- Tastet, J.-P., Pontee, N.I., 1998. Morpho-chronology of coastal dunes in Médoc. A new interpretation of Holocene dunes in Southwestern France. *Geomorphology* 25, 93–109.
- Trigo, R.M., DaCamara, C.C., 2000. Circulation weather types and their influence on the precipitation regime in Portugal. *International Journal of Climatology* 20, 1559–1581.
- Trigo, R.M., Osborn, T.J., Corte-Real, J.M., 2002. The North Atlantic Oscillation influence on Europe: climate impacts and associated physical mechanisms. *Climate Research* 20, 9–17.
- Trigo, R.M., Pozo-Vázquez, D., Osborn, T.J., Castro-Díez, Y., Gámiz-Fortis, S., Esteban-Parra, M.J., 2004. North Atlantic oscillation influence on precipitation, river flow and water resources in the Iberian Peninsula. *International Journal of Climatology* 24, 925–944.
- Trigo, R., Xoplaki, E., Zorita, E., Luterbacher, J., Krichak, S.O., Alpert, P., Jacobeit, J., Sáenz, J., Fernández, J., González-Rouco, F., Garcia-Herrera, R., Rodo, X., Brunetti, M., Nanni, T., Maugeri, M., Türkeş, M., Gimeno, L., Ribera, P., Brunet, M., Trigo, I.F., Crepon, M., Mariotti, A., 2006. Relations between variability in the Mediterranean Region and mid-latitude variability. In: Lionello, P., Malanotte-Rizzoli, P., Boscolo, R. (Eds.), *Mediterranean Climate Variability*. Elsevier, Amsterdam, pp. 179–226.
- Trigo, R.M., Valente, M.A., Trigo, I.F., Miranda, P.M.A., Ramos, A.M., Paredes, D., García-Herrera, R., 2008. The impact of North Atlantic wind and cyclone trends on European precipitation and significant wave height in the Atlantic. *Annals of the New York Academy of Sciences* 1146, 212–234.
- Trouet, V., Esper, J., Graham, N.E., Baker, A., Scourse, J.D., Frank, D.C., 2009. Persistent positive North Atlantic oscillation mode dominated the medieval climate anomaly. *Science* 324, 78–80.
- Trouet, V., Scourse, J.D., Raible, C.C., 2012. North Atlantic storminess and Atlantic meridional overturning circulation during the last millennium: reconciling contradictory proxy records of NAO variability. *Global and Planetary Change* 84–85, 48–55.
- Tsoar, H., Levin, N., Porat, N., Maia, L.P., Herrmann, H.J., Tatumi, S.H., Claudino-Sales, V., 2009. The effect of climate change on the mobility and stability of coastal sand dunes in Ceará State (NE Brazil). *Quaternary Research* 71, 217–226.
- Uppala, S.M., Källberg, P.W., Simmons, A.J., Andrae, U., Bechtold, V.D.C., Fiorino, M., Gibson, J.K., Haseler, J., Hernandez, A., Kelly, G.A., Li, X., Onogi, K., Saarinen, S., Sokka, N., Allan, R.P., Andersson, E., Arpe, K., Balmaseda, M.A., Beljaars, A.C.M., Berg, L.V.D., Bidlot, J., Bormann, N., Caires, S., Chevallier, F., Dethof, A., Dragosavac, M., Fisher, M., Fuentes, M., Hagemann, S., Hólm, E., Hoskins, B.J., Isaksen, I., Janssen, P.A.E.M., Jenne, R., McNally, A.P., Mahfouf, J.F., Morcrette, J.J., Rayner, N.A., Saunders, R.W., Simon, P., Sterl, A., Trenberth, K.E., Untch, A., Vasiljevic, D., Viterbo, P., Woollen, J., 2005. The ERA-40 re-analysis. *Quarterly Journal of the Royal Meteorological Society* 131, 2961–3012.
- Vicente-Serrano, S.M., López-Moreno, J.J., 2008. The nonstationary influence of the North Atlantic oscillation on European precipitation. *Journal of Geophysical Research* 113, D20120. doi:10.1029/2008JD010382.
- Vicente-Serrano, S., Trigo, R., López-Moreno, J.J., Liberato, M.L.R., Lorenzo-Lacruz, J., Beguería, S., Morán-Tejada, E., Kenawy, A.E., 2011. Extreme winter precipitation in the Iberian Peninsula in 2010: anomalies, driving mechanisms and future projections. *Climate Research* 46, 51–65.
- Vis, G.-J., Bohncke, S.J.P., Schneider, H., Kasse, C., Coenraads-Nederveen, S., Zuurbier, K., Rozema, J., 2010. Holocene flooding history of the lower Tagus valley (Portugal). *Journal of Quaternary Science* 25, 1222–1238.
- Wanner, H., Brönnimann, S., Casty, C., Gyalistras, D., Luterbacher, J., Schmutz, C., Stephenson, D.B., Xoplaki, E., 2001. North Atlantic oscillation – concepts and studies. *Surveys in Geophysics* 22, 321–381.
- Wanner, H., Beer, J., Bütikofer, J., Crowley, T.J., Cubasch, U., Flückiger, J., Goosse, H., Grosjean, M., Joos, F., Kaplan, J.O., Küttel, M., Müller, S.A., Prentice, I.C., Solomina, O., Stocker, T.F., Tarasov, P., Wagner, M., Widmann, M., 2008. Mid- to Late Holocene climate change: an overview. *Quaternary Science Reviews* 27, 1791–1828.
- Wilson, P., Orford, J.D., Knight, J., Braley, S.M., Wintle, A.G., 2001. Late-Holocene (post-4000 years BP) coastal dune development in Northumberland, northeast England. *The Holocene* 11, 215–229.
- Wilson, P., McGourty, J., Bateman, M.D., 2004. Mid-to late-Holocene coastal dune event stratigraphy for the north coast of Northern Ireland. *The Holocene* 14, 406–416.
- Wintle, A.G., Murray, A.S., 2006. A review of quartz optically stimulated luminescence characteristics and their relevance in single-aliquot regeneration dating protocols. *Radiation Measurements* 41, 369–391.
- Wolfe, S.A., David, P.P., 1997. Parabolic dunes: examples from the Great sand Hills, southwestern Saskatchewan. *Canadian Geographer/Le Géographe Canadien* 41, 207–213.
- Zazo, C., Mercier, N., Silva, P.G., Dabrio, C.J., Goy, J.L., Roquero, E., Soler, V., Borja, F., Lario, J., Polo, D., de Luque, L., 2005. Landscape evolution and geodynamic controls in the Gulf of Cadiz (Huelva coast, SW Spain) during the Late Quaternary. *Geomorphology* 68, 269–290.
- Zeeberg, J., 1998. The European sand belt in eastern Europe – and comparison of Late Glacial dune orientation with GCM simulation results. *Boreas* 27, 127–139.